Experimental and Density Functional Theory on L-Histidine Hydrofluoride: A Nonlinear Optical Single Crystal.

K. Deepa[1], N. Indumathi[2], S. Senthil[2], M. Victorantonyraj[1], and J. Madhavan[1]*.

[1]Department of Physics, Loyola College, Chennai, India.
[2]Department of Physics, Government Arts College for Men, Nandanam, Chennai, India.

ABSTRACT

Single crystals of L-histidine Hydrofluoride (LHHF) have been successfully grown by slow solvent evaporation technique at room temperature. Powder X-Ray diffraction patterns has been recorded and indexed for the analysis of crystalline nature and the lattice parameters of the grown crystals. The non-centro symmetric single crystal of L- Histidine Hydrofluoride (LHHF) was crystallizes in orthorhombic crystal system with space group $P2_12_12_1$, it exhibit second order non-linear optical (NLO) susceptibility due to the intermolecular charge transfer. The functional groups are identified by Fourier transform infrared spectral analysis and compared with theoretical spectrum. The optical transmission range of the LHHF crystal has measured by UV–Vis–NIR studies. It is observed that the minimum absorption in the entire visible and ultra violet range of 240–1500 nm. From absorption spectra the optical band gap is found to be 4.89 eV. Theoretically Simulated XRD pattern of LHHF single crystal has been carried out. Vibration frequencies are calculated using B3LYP/6-31+G(d,p) and B3LYP/6-311++ G(d, p) . Vibration mode assignments were also compared with the experimental results. The optimized geometrical parameters, fundamental vibrational frequencies, IR intensity, Raman activity, atomic small charges, dipole moment, reduced mass, force constant and other thermodynamic parameters were calculated. The second harmonic generation (SHG) efficiency has been carried out and it reveals the NLO property of the crystals. The HOMO and LUMO analysis were used to determine the charge transfer within the molecule and quantum chemical parameters related to the LAO compound.

Keywords: Powder XRD, optical absorption, Density Functional Theory, HOMO-LUMO analysis, FTIR, SHG efficiency.

*Corresponding author

INTRODUCTION

Intensive research effort has been concerted on the investigation of the nonlinear optical processes in π-conjugated organic molecules and materials in the recent past decades [1, 2]. The rapid and sustained growth of the field is mainly due to the technological promise of these materials. The utmost importance in the design strategy for efficient non-linear optical (NLO) materials in terms of the molecular design and the supramolecular aggregation is basically aimed to accomplish their potential applications in various photonic technologies. This overwhelming approach crafts a sole field of intriguing explorations in chemical synthesis, molecular and material characterization, theoretical modeling, and NLO studies and photonics technology [3]. The molecular NLO active crystals have been intensively studied to establish the observed structure function correlation through the computational modeling of molecules as the origin of the nonlinear optical response in such systems are governed by the electronic polarizability of the electrons at the molecular level [4] as well as the geometrical arrangement of the NLO-chromophores present in the molecular system. The sensitive understanding of the structural and electronic response properties of NLO materials have been provided extensively both experimentally and theoretically using the quantum mechanical density functional theory (DFT) approach by vibrational spectroscopy. The molecular structural properties such as their atomistic level energy, vibrational frequencies, transition moment directions, magnitudes of the normal modes of vibrations etc. can be simulated with great accuracies by theoretical computational methods. Considerable effort has been devoted to understand the vibrational, optical, nonlinear response and electronic structure properties of the molecule- based NLO active organic crystals by the DFT based quantum chemical analysis [5]. In this paper, we report the synthesis, crystal structure, spectral and DFT studies of L- Histidine Hydrofluoride (LHHF) single crystals. Here the structural properties of the title compound were studied experimentally and is compared theoretically. Thus, owing to the industrial and biological significance of substituted quinolines, extensive spectroscopic studies on using Fourier transform infrared (FTIR) and NMR. The DFT calculations with the hybrid exchange-correlation functional B3LYP (Becke's three parameter (B3) exchange in conjunction with the Lee–Yang–Parr's (LYP) correlation functional) which are specifically significant in systems comprising of extensive electron conjugation and/or electron lone pairs [6-9]. Therefore the present investigation has been undertaken to study the vibrational spectra of this molecule entirely and to classify the various modes with greater wave number accuracy. Also, chemical reactivity values such as chemical hardness, chemical potential electro negativity and electrophilicity index. HOMO, LUMO analysis have been used to reveal information regarding charge transfer within the molecule.

SYNTHESIS AND GROWTH

From aqueous solution with equimolar proportion of L-histidine and Hydrofluoric acid the product compound L-His.HF.2H_2O is formed. The solubility of LHHF was measured at 30, 35, 40, 45, 50 and 55 °C and the variation of solubility with temperature is shown in Figure.1. The solution was saturated at 40 °C and seed crystals were formed due to spontaneous nucleation. Transparent and good quality seed crystals were used for growth experiments. Single crystals of size 33 x 7 x 11 mm^3 were grown in 50 days and the photograph of the as grown crystal of LHHF is shown in Figure.2.
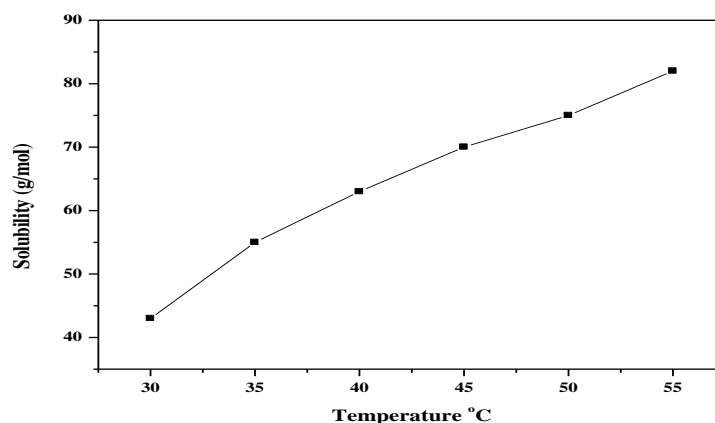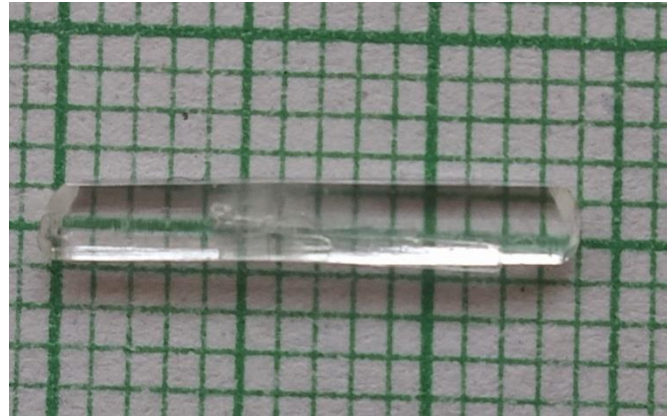

Figure.1 Solubility curve of LHHF crystal

Figure .2 Photograph of as grown LHHF

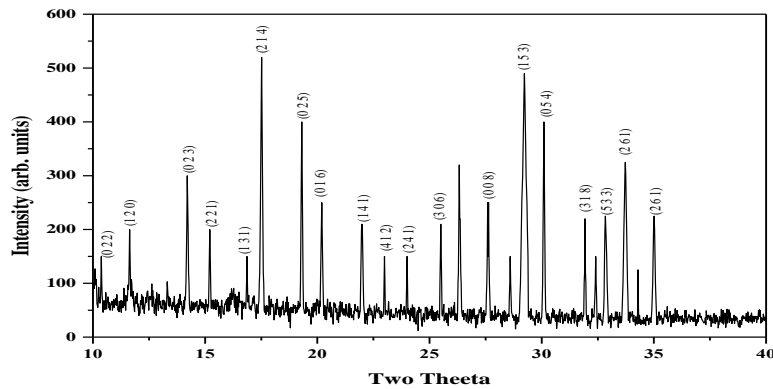**RESULTS AND DISCUSSION**

POWDER X-RAY DIFFRACTION

Figure.3 Experimentally obtained Powder XRD pattern of LHHF
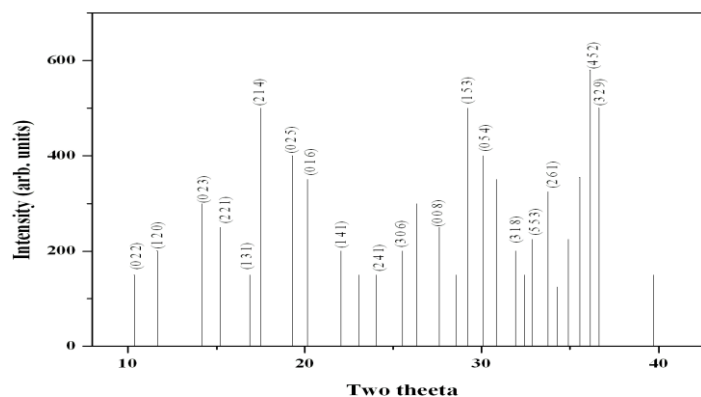

Figure.4 Theoretically simulated powder XRD pattern of LHHF

The crystal structure and purity of L-histidine Hydrofluoride (LHHF) was confirmed by X-ray diffraction measurement. It is observed that L-Histidine Hydrofluoride (LHHF) crystallizes in the orthorhombic crystal system with the space group $P2_12_12_1$ suggesting that the crystal is non Centro symmetric nature which supports one of the basic requirements for non linear optical response of the crystal. The calculated unit cell parameters are a = 8.449(2) Å, b = 8.572(3) Å, c = 13.895(4) Å and unit cell volume V=1006.343(3) Å^3. The

obtained lattice parameters are in good agreement with the reported values [10]. The indexed powder XRD pattern of the as-grown LHHF is shown in Figure. 3. The sample is of single phase without any detectable impurity and narrow peaks indicate the good crystallinity of the material. Theoretically Simulated XRD pattern of LHHF single crystal with indexed peak is given in Figure.4. Most of the peak positions in powder XRD coincides with the simulated pattern.

COMPUTATIONAL DETAILS

Density functional theory calculations are performed using Gaussian'03 program package [11]. The geometries were fully optimized without any constraint. The vibration frequencies are calculated by using B3LYP/6-31+G(d, p) and B3LYP/6-311++ G(d, p) respectively. Vibration mode assignments were also compared with the experimental results. The optimized geometrical parameters, fundamental vibrational frequencies, IR intensity, Raman activity, atomic small charges, dipole moment, reduced mass, force constant and other thermodynamic parameters were calculated.

MOLECULAR GEOMETRY

The numbering scheme for L- Histidine Hydrofluoride is shown in Figure.5. The most optimized structural parameters were calculated and were depicted in Table.1 and 1(a). Generally the bond lengths and bond angles depend on the method and the basis set used in the calculations, and they can be used as foundation to calculate the molecular properties for the compounds. The global minimum energy was obtained by DFT methods with different basis sets (such as 6-31+G (d, p), 6-311++G (d, p)) as -797.851325 a. u and -798.12081120 a. u respectively.

Parameters	B3LYP	
	6-31+ G (d, p)	6-311++ G (d, p)
Bond length in (Å)		
C_2-C_3	1.37881	1.37497
C_3-N_6	1.38631	1.38548
N_6-C_1	1.33189	1.33084
C_1-N_5	1.35827	1.35602
C_3-C_{10}	1.47612	1.47478
C_{10}-C_{13}	1.52657	1.52798
C_{13}-C_{15}	1.54942	1.54280
C_{15}-O_{16}	1.26398	1.26308
C_{15}-O_{17}	1.29078	1.28826
C_{13}-N_{18}	1.48598	1.48452
N_{18}-H_{21}	1.02841	1.02557
N_{18}-H_{19}	1.18604	1.15265
N_{18}-H_{20}	1.07359	1.07430
O_{22}-H_{24}	1.10888	1.08154
O_{23}-H_{26}	0.97889	0.97357
O_{23}-H_{27}	1.03897	1.03206
F_{28}-H_{27}	1.43141	1.43645
F_{28}-H_{24}	1.26216	1.29897

Table.1 Selected bond lengths of LHHF molecule

	B3LYP	
Parameters	6-31+ G (d, p)	6-311++ G (d, p)
Bond Angles in (°)		
C_2-C_3-N_6	108.17010	108.09252
C_3-N_6-C_1	108.90639	108.98840
C_1-N_5-C_2	110.25494	110.29489
N_5-C_2-C_3	105.07825	105.15775
C_2-C_3-C_{10}	128.89605	129.94414
C_3-C_{10}-C_{13}	114.90015	112.80176
C_{10}-C_{13}-N_{18}	110.77033	112.55345
C_{10}-C_{13}-C_{15}	114.69248	112.47560
N_{18}-C_{13}-C_{15}	104.70545	105.20213
C_{13}-C_{15}-O_{16}	116.18047	116.05654
C_{13}-C_{15}-O_{17}	117.80736	117.66739
H_9-C_2-C_3	127.00646	128.64119
H_9-C_2-N_5	127.90197	126.13612
H_{26}-O_{23}-H_{27}	110.85428	113.24704
H_{24}-O_{22}-H_{25}	118.71690	116.62630
H_{21}-N_{18}-H_{20}	111.03692	108.97038
H_{11}-C_{10}-H_{12}	105.89538	106.66584

Table .1 (a) selected bond angles of LHHF molecule
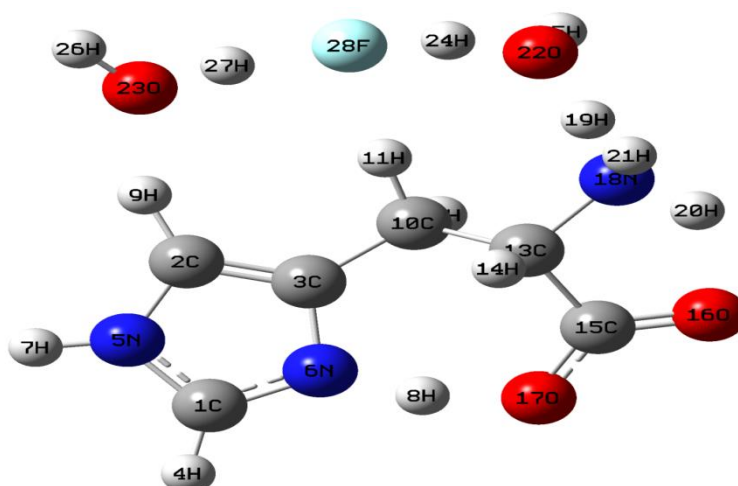

Figure.5. Atomic numbering system adapted for ab initio computations of LHHF molecule.

VIBRATIONAL ANALYSIS

The FT-IR spectra of LHHF, was recorded on BRUKER IFS 66V FT-IR spectrometer using KBr pellet in the range 4000 cm^{-1} to 400 cm^{-1}. The observed FT-IR and theoretically stimulated FT-IR spectrum is shown in Figures.6, 7 and 8 respectively. The detailed vibrational assignments of fundamental modes of LHHF along with the FT-IR experimental frequencies, reduced mass, force constant and spectral assignments are shown in Table .2. The title molecule LHHF has 28 atoms. It has 78 normal vibrational modes. 53 of these modes are in-plane symmetric (A') and 25 out-of-plane symmetric (A") with respect to the reflection on the symmetry plane.Γ_{78} = 53 A' (in-plane) + 25 A"(out-of-plane) respectively The theoretical and experimental wave numbers are in fair agreement and the assignments of wave numbers for different functional groups are discussed below.

| Experimental Frequency (cm^{-1}) | Observed | | | | | | Assignments |
| | B3LYP/6-31+G(d,p) | | | B3LYP/6-311++G(d,p) | | | |
	FTIR frequency	Reduced mass	Force constant	FTIR frequency	Reduced mass	Force constant	
	3752.0585	1.0660	8.8423	3746.3462	1.0663	8.8178	OH st
	3695.7544	1.0656	8.5753	3725.0380	1.0666	8.7203	OH st
	3600.5541	1.0821	8.2656	3580.4480	1.0829	8.1793	OH st
	3466.1981	1.0734	7.5986	3443.9726	1.0725	7.4946	NH$_2$ sym st
3138.92	3273.3514	1.1017	6.9552	3227.5591	1.1025	6.7665	CH$_2$ asy st
3021.83	3005.4301	1.0864	5.7818	2987.7944	1.0863	5.7135	CH st
	2984.4402	1.0875	5.7072	2962.5370	1.0896	5.6345	CH st in CH$_3$
	2923.4370	1.0610	5.3425	2903.2074	1.0608	5.2677	CH st in CH$_3$
2875.48	2845.6892	1.0641	5.0771	2817.2803	1.0693	5.0004	CH$_3$ sym st
	2817.3858	1.0786	5.0441	2786.3661	1.0639	4.8664	CH st
2699.52	2681.9047	1.1242	4.7642	2620.8154	1.1410	4.6176	CH st
2142.72	2137.2235	1.0554	2.8404	2244.8411	1.0614	3.1515	CN st
	1847.0101	1.1703	2.3522	1910.8366	1.1554	2.4856	NH$_2$ sci
	1781.4849	1.0782	2.0161	1811.2720	1.1073	2.1403	NH$_2$ st
1715	1748.3303	3.2182	5.7958	1723.2240	1.3890	2.4301	C OO$^-$ ast
	1686.4142	1.1194	1.8757	1698.1975	1.7618	2.9936	C=N st
1630.32	1631.9540	1.3554	2.1268	1642.8654	1.0839	1.7237	H$_2$O
	1626.0919	1.9451	3.0302	1629.9839	1.8967	2.9690	C=C st
1608.06	1622.2299	1.0431	1.6173	1607.2471	1.1274	1.7159	NH$_2$ sci
	1583.0846	1.3426	1.9825	1593.1442	1.6561	2.4765	CH$_2$ ipb
1535.49	1531.3074	3.1293	4.3233	1521.2012	2.7257	3.7163	COO$^-$ asy
	1505.1341	1.1811	1.5765	1496.9365	1.1833	1.5622	C=C st
1469.62	1465.5626	1.9695	2.4924	1469.8037	1.1653	1.4832	CH3 asy de
	1457.7539	1.5386	1.9264	1454.9756	2.1788	2.7175	CH ipb
1411.08	1430.3205	1.2799	1.5428	1432.7734	1.5489	1.8734	COO$^-$ sym
	1386.6427	2.3404	2.6513	1373.6022	1.6258	1.8073	CH opb
1359.86	1360.4303	1.7678	1.9277	1364.1394	2.3791	2.6084	COO$^-$ ipb
	1349.7423	2.7285	2.9287	1344.8845	1.8054	1.9239	CC st
1337.40	1336.8213	1.9227	2.0245	1323.5279	1.6850	1.7390	CO st
	1318.3830	1.6260	1.6651	1308.2663	1.7957	1.8109	CO st
1286.68	1280.5158	1.4886	1.4381	1292.5885	2.1535	2.1199	δ COO$^-$
	1267.5543	1.1110	1.0517	1272.8865	1.1335	1.0820	OH ipb
	1264.5989	1.3740	1.2946	1243.7041	1.4786	1.3475	OH ipb
1242.77	1233.3235	1.8013	1.6143	1225.9543	1.8859	1.6700	ν CN
	1191.0341	1.1957	0.9994	1186.5976	1.2220	1.0138	CH$_2$ roc
	1164.6934	1.4057	1.1235	1168.2615	1.3975	1.1238	γ NH$_3$
	1139.2063	1.0891	0.8328	1123.8078	1.7028	1.2671	PhI
1125.63	1123.2150	1.5203	1.1301	1111.9045	1.7277	1.2585	CN st
	1113.6236	1.7940	1.3108	1087.4235	3.3531	2.3361	OH ipb
1074.46	1093.5384	3.0164	2.1253	1073.9223	1.1082	0.7531	OH ipb
	1040.0327	1.2239	0.7800	1048.7703	1.1875	0.7696	PhI
	1034.0918	2.5038	1.5775	1008.9146	2.4627	1.4769	δ CH
	985.6891	1.8474	1.0575	975.7703	2.6733	1.4996	CH opb
	976.5422	3.0552	1.7166	960.6483	2.3357	1.2700	R asyd
	948.2419	1.0980	0.5817	910.7856	2.7565	1.3472	γ CN
906.14	916.3631	3.4301	1.6970	900.4025	1.0997	0.5253	γ CC
811.01	827.5760	3.7957	1.5317	821.1376	4.5337	1.8011	CH opb
	777.8033	1.5363	0.5476	780.8596	1.6036	0.5761	R berth
	771.6305	2.7721	0.9725	763.0730	3.1572	1.0831	γ CH
	749.5044	1.3736	0.4546	731.5979	2.2424	0.7072	CN opb

	735.3645	2.6740	0.8520	724.0622	1.7072	0.5273	Γ OCC
	726.2427	1.6119	0.5009	708.8697	1.4798	0.4381	CH opb
679.29	675.2904	3.1951	0.8584	667.1351	2.6357	0.6912	C-C b
	656.8500	2.6728	0.6794	653.0995	2.4815	0.6236	NH b
	652.0028	3.1025	0.7771	647.4530	3.8294	0.9458	C-H opb
620.75	617.9157	4.0433	0.9096	606.1041	4.8120	1.0415	C-H opb
	568.5141	2.2642	0.4312	559.1203	3.5932	0.6618	NH_2 wag
532.93	557.7985	1.4038	0.2573	540.1518	1.2205	0.2098	H_2O
	504.1990	2.2676	0.3396	489.2668	1.3607	0.1919	C-CO ipb
	480.5358	2.0653	0.2810	451.5125	2.6248	0.3153	C-C b
	408.4138	3.4158	0.3357	399.2128	3.2990	0.3098	II Ph tor
	396.8972	4.9820	0.4624	380.8780	5.0316	0.4301	CH st
	381.7843	5.2813	0.4536	344.5164	5.2943	0.3702	C-C b
	340.4415	5.6518	0.3859	335.0753	5.5452	0.3668	C-H
	318.9529	4.5983	0.2756	314.8048	4.8999	0.2861	CC ipd
	308.6586	3.8516	0.2162	299.5251	3.3724	0.1783	CC ipd
	257.7350	3.5772	0.1400	267.2962	4.7462	0.1998	COO⁻
	232.8291	3.7562	0.1200	244.9069	1.2112	0.0428	NH_2 tor
	221.9683	1.2638	0.0367	234.5763	3.8551	0.1250	CO opb
	172.0219	2.2461	0.0392	156.5012	4.2898	0.0619	CN ipb
	155.2562	3.5493	0.0504	142.4993	4.9304	0.0590	CCC st
	148.9751	9.3720	0.1225	129.0500	3.5074	0.0344	C-C-N ipb
	125.8664	3.6873	0.0344	116.7456	2.3733	0.0191	C-C-N ipb
	110.8900	6.8099	0.0493	92.0818	4.6797	0.0234	CC ipb
	80.3693	4.9585	0.0189	73.6147	4.0756	0.0130	CNH_2 t
	66.2734	4.4976	0.0116	51.0051	6.5242	0.0100	CNH_2 t
	60.4825	6.3150	0.0136	33.5042	4.4752	0.0030	NH_2 tor

St-stretching ; **sym st**- symmetry stretching ;**asy st**- assymtry stretching ; **sci**-scisorring **t**-twisting ;**ipb**-in-planebending ;**opb**- out-of-plane bending; **ipd**-inplane deformation **wag**- wagging; **R**-anthracene ring;; **roc**-rocking;

Table .2.Experimental and Calculated B3LYP/6-31+&6-311++ levels of vibrational frequencies of LHHF
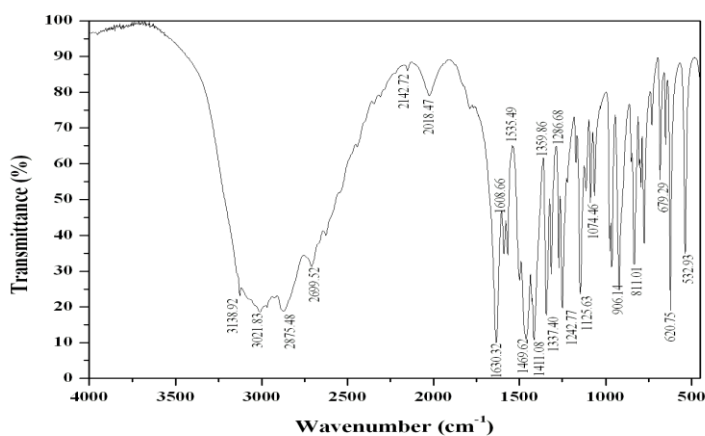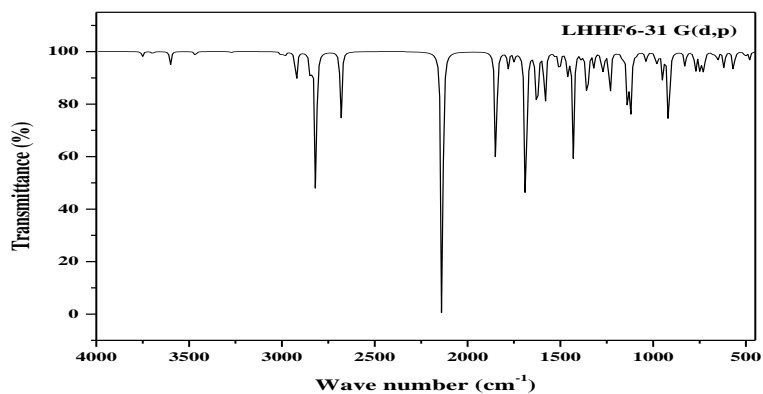

Figure.6. Experimental FT-IR Spectrum of LHHF

Figure.7. Observed FT IR Spectrum of LHHF by 6-31+ G (d, p) method

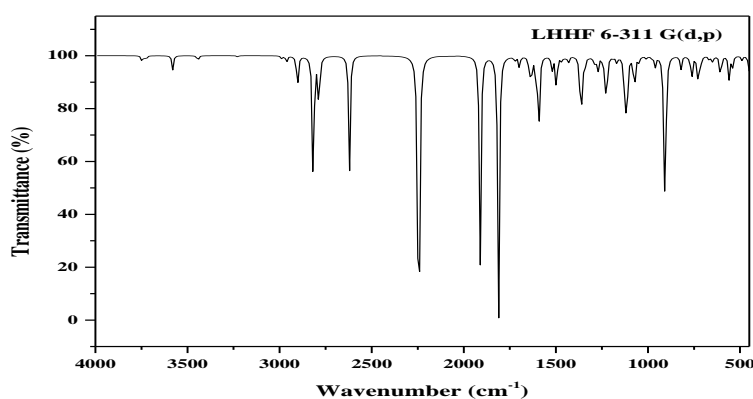**Figure .8. Observed FT IR Spectrum of LHHF by 6-311++ G (d, p) method**

WATER MOLECULES

Basically, water has two OH stretching modes (around 3600 cm^{-1}) and one bending mode around 1630 cm^{-1}. From LHHF it is observed that 1630.32 cm^{-1} from IR and 1631.95, 1642.86cm^{-1}from the computed values using DFT basis sets.The corresponding bands are strong in the IR. Lower frequency IR modes of water below 600 cm^{-1} could arise from librational modes, but they overlap also with other bands and cannot be clearly assigned here.

H- F VIBRATIONS

The H- Fhydrogen-bonded complex has been the subject of many experimental and theoretical studies. The gas phase structure of this complex was determined by pulsed-nozzle Fourier transform microwave spectroscopy. The infrared spectra in low temperature argon matrices clearly showed that the H-Fcomplex exists in the molecular form. Moreover, molecular properties like structure and energy of interaction of this complex were the subject of very intensive quantum chemical studies at the nonempirical level of calculations. According to the symmetry adopted perturbation theory (SAPT) analysis the nature of this interaction is mainly induction with non-negligible contribution of exchange term.

COO$^-$VIBRATIONS

Carboxyl group vibrations give rise to intense characteristic bands due to conjugation or formation of hydrogen bonds. These stretching and bending vibrations of acid group are generally expected in the region 1400–1200 cm^{-1}.The presence of strong absorption bands at 1411.08, 1286.68 cm^{-1} confirmed the presence of

COO⁻groups by IR and 1430.32, 1432.77 using 6-31+ G (d, p) and 1233.32, 1225.95 cm⁻¹ using 6-311++ g (d, p) basis sets. The in-plane O-H deformation vibration usually appears as strong band in the region 1440-1260 cm⁻¹.The strong experimentally predicted band at 1359 cm⁻¹ is assigned to in-plane bending vibration of COO⁻ group for the title molecule and it is in good agreement at 1360, 1364.13 cm⁻¹ in computed FTIR spectrum.

Force constants and reduced masses for IR frequencies of LHHF molecule are calculated. Force constant can be correlated with bond length and are essential for discussing the strength of the bonds then the variation in bond length is attributed to charge transfer capacity of the molecule which is a vital parameter for NLO behavior.

HYPERPOLARIZABILITY STUDIES

Theoretical calculations on molecular hyperpolarizability become one of the key factors in the second-order NLO materials. Theoretical determination of hyperpolarizability provides a guideline to experimentalists for the design and synthesis of organic NLO materials. Nonlinearity inorganic chromophores can be synthetically modulated by varying the composition or length of conjugated p-systems, and by evaluating the effects of various electron-donor and electron-acceptor groups. First order hyperpolarizability values are given in table.3.

Para	B3LYP/ 6-31+G	B3LYP/6-311++G
Dipole moment in debye		
μ_x	-5.3475	-5.0500
μ_y	-0.1661	-0.3095
μ_z	1.7402	0.8309
μ_{tot}	5.6260	5.1272
Polarizability in esu		
α_{xx}	102.52545	139.47847
α_{xy}	34.845246	-5.908715
α_{yy}	84.731604	65.072695
α_{xz}	12.151241	6.3422019
α_{yz}	-1.5616698	-2.236005
α_{zz}	113.808075	121.98602
α_o	0.8399×10^{-30}	0.91096×10^{-30}
Hyperpolarizability in esu		
β_{xxx}	-269.862498	-217.36375
β_{xxy}	-253.719608	-251.23383
β_{xyy}	-122.858369	-189.148803
β_{yyy}	-183.92514	-165.304903
β_{xxz}	139.317521	103.2400168
β_{xyz}	-101.0015581	-114.314853
β_{yyz}	111.661742	161.5513002

β_{xzz}	-147.655807	-140.921474
β_{yzz}	1.015538	1.7805245
β_{zzz}	-352.23228	-361.372294
β_{tot}	5.91506×10^{-30}	5.80467×10^{-30}

Table .3. The electric dipole moment μ, the average polarizability α_{tot} and First hyperpolarizability β_{tot} for LHHF

They determine not only the strength of molecular interactions (long-range interaction, dispersion force, etc.) and the cross sections of different scattering and collision process but also the NLO properties of the system. LHHF is an excellent NLO material which is understood from the values of hyperpolarizability.

HOMO-LUMO GAP

Figure.9 and10 shows the highest occupied molecular orbital (HOMO) and lowest unoccupied molecular orbital (LUMO) of LHHF. In order to evaluate the energetic behavior of LHHF, the energies of HOMO and LUMO their orbital energy gaps using B3LYP/ 6-31+G (d,p) and 6-311++ G (d, p) sets are calculated. The frontier orbital gap facilitates in characterizing the chemical reactivity and kinetic stability of the molecule. The red and green colors represent the positive and negative values for the wave function. The HOMO is the orbital that primarily acts as an electron donor and the LUMO is the orbital that mainly acts as an electron acceptor. The electronic absorption corresponds to the transition from the ground to the first excited state and is mainly described by one electron excitation from the highest occupied molecular orbital (HOMO) to the lowest unoccupied molecular orbital (LUMO). While the energy of the HOMO is directly related to the ionization potential, LUMO energy is directly related to the electron affinity.

LUMO PLOT (First excited State)

$E_{LUMO} = -0.11736$

$\Delta E = -0.15354$ a.u
$\Delta E = 4.178$ eV

$E_{HOMO} = 0.13618$

HOMO PLOT (Ground State)
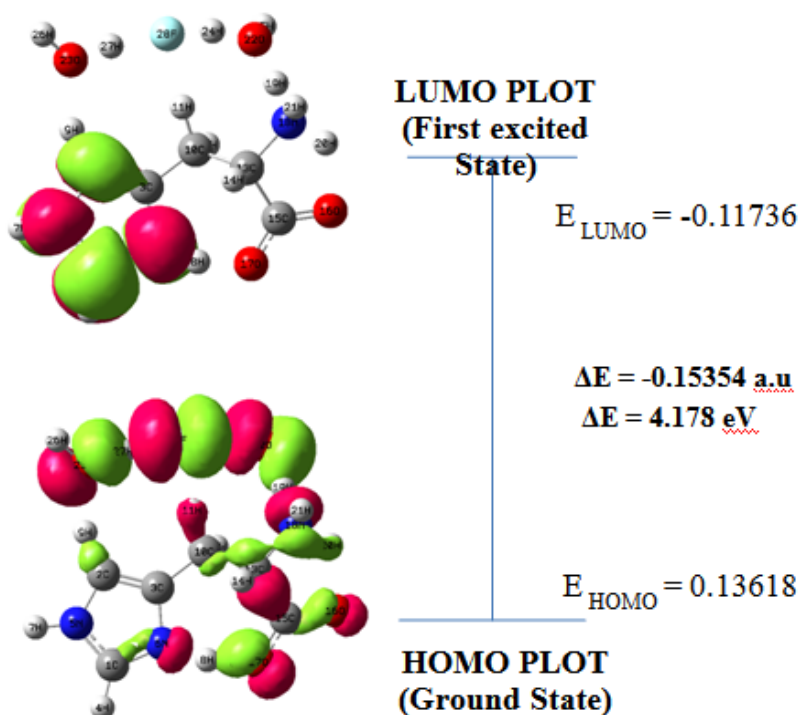
Figure .9. HOMO –LUMO plot of LHHF at B3LYP/6-31+G(d,p)

LUMO PLOT
(First excited State)

$E_{LUMO} = -0.07872$

$\Delta E = -0.15657$ a.u

$\Delta E = 4.260$ eV

$E_{HOMO} = -0.23529$
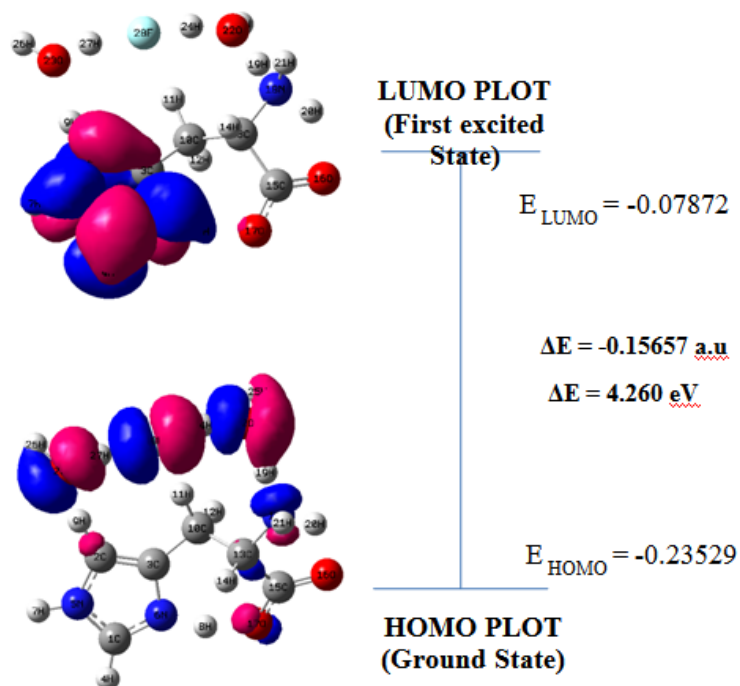
HOMO PLOT
(Ground State)

Fig .10. HOMO –LUMO plot of LHHF at B3LYP/6-311++G(d,p)

THERMODYNAMIC PROPERTIES

Theoretical geometrical parameters represent a good approximation and they are the basis for calculating vibrational frequencies and thermodynamic parameters. These functions describe the thermodynamic stability of system at given conditions of pressure and temperature. In order to study energetic, structural and reactivity of the title molecule, some of the vibrational and thermodynamic parameters (such as zero point vibrational energy, thermal energy, specific heat capacity, rotational constants, entropy) of LHHF by DFT with 6-31+ G (d, p) and 6-311++ G (d, p) basis sets have been presented in Table .4.

Parameters	B3LYP	
	6-31+ G (d, p)	6-311+++ G (d,p)
Zero Point Vibrational Energy	136.87951	135.95896
Rotational Constants		
A	0.61383	0.61650
B	0.54455	0.53406
C	0.29944	0.29461
Thermal energy		
Total	146.555	145.334
Translational	0.889	0.889
Rotational	0.889	0.889
Vibrational	144.777	143.556
Molar capacity at constant Volume		
Total	56.735	55.476
Translational	2.981	2.981
Rotational	2.981	2.981
Vibrational	50.773	49.515

Entropy			
Total	125.363	123.304	
Translational	41.945	41.945	
Rotational	32.441	32.472	
Vibrational	50.977	48.887	

Table .4. Theoretically computed Zero point vibrational energy (kcal mol^{-1}), rotational constants (GHz), thermal energy (kcal mol^{-1}), molar capacity at constant volume (cal mol^{-1} Kelvin^{-1}) and entropy (cal mol^{-1}Kelvin^{-1})

MULLIKEN POPULATION ANALYSIS

The atomic charge in molecules is fundamental to chemistry. The charge distribution on the molecule has an important role in the application of quantum mechanical calculations for the molecular system. Atomic charge affects dipole moment, polarizability, electronic structure and other molecular properties of the system. Mulliken charges are calculated by determining the electron population of each atom as defined in the basic functions. The charge distributions calculated by the Mulliken [12]. The Mulliken atomic charges of title molecule calculated by DFT method at 6-311++G(d,p) basic set in gaseous phase are given in Table 5.The results show that all the hydrogen atoms in the molecules lost electrons, the nitrogen atom and the fluorine atoms in molecules accepted electrons and the carbon atomic charges were found to be both positive and negative values.

Atom Number	Mulliken atomic Charges - B3LYP		Atom Number	Mulliken atomic Charges - B3LYP	
	6-31+ G(d, p)	6-311++ G(d, p)		6-31+ G(d, p)	6-311++ G (d, p)
C_1	0.171223	-0.131397	C_{15}	0.396935	-0.004712
C_2	0.135020	-0.166808	C_{16}	-0.51470	-0.185833
C_3	0.097474	-0.106028	C_{17}	-0.47342	-0.365548
C_4	0.178750	-0.127766	H_{18}	-0.71006	0.237748
C_5	-0.61479	-0.095515	C_{19}	0.398499	-0.027154
C_6	-0.60822	-0.176388	H_{20}	0.379407	0.173321
H_7	0.353573	0.167451	H_{21}	0.382567	0.192087
H_8	0.347622	0.166995	Cl_{22}	-0.70785	-0.018841
H_9	0.219004	0.190036	O_{23}	-0.64823	-0.441811
H_{10}	-0.25411	0.201625	N_{24}	0.388365	-0.936045
H_{11}	0.186976	0.167394	H_{25}	0.354228	0.334891
C_{12}	0.248915	0.283355	H_{26}	0.343826	0.387383
C_{13}	-0.13537	-0.161824	H_{27}	0.361862	0.378965
C_{14}	0.155482	0.443386	F_{28}	-0.43292	-0.415960

Table .5. Mulliken Population analysis of LHHF at B3LYP methods with 6-31+&6-311++ basis sets

UV-VIS-NIR SPECTRUM ANALYSIS

The optical absorption spectral analysis of the LHHF single crystal was carried out between 240 and 1500 nm using VARIAN CARY 5E spectrophotometer and is shown in the Figure.11. As the crystal is colorless, there is very low absorbance in the entire visible region and shows maximum absorption at UV region. This is one of the most desirable properties of the crystals for the device fabrication. A good optical transmittance is very desirable in an NLO crystal since the absorptions, if any, in an NLO material near the fundamental of the second harmonic will lead to less conversion efficiency in those wavelengths. As the entire visible region does not bear any absorption band it can be used for NLO applications. The values of the optical band gap E_g were obtained from the intercept of $(\alpha h\nu)^2$ versus $h\nu$ curve plotted in   Figure .12. Energy gap (E_g) was evaluated

by extrapolating the linear part of the curve to energy axis. The band gap is found to be 4.89 eV. Extinction coefficient, reflectance, refractive index, complex dielectric constants, optical conductivity and electrical conductivity with photon energy as a function of incident photon energy for the grown single crystal are illustrated in Figures.13 to18. It is shown that the refractive index and extinction coefficient of LHHF changes with increasing photon energy. The low extinction coefficient (10^{-5}) and high optical conductivity (10^9) confirms the high photo response nature of the material.
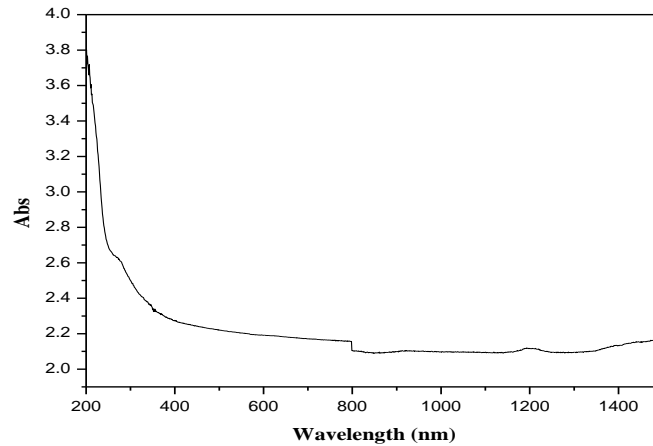
Figure .11. Optical absorption spectrum of LHHF
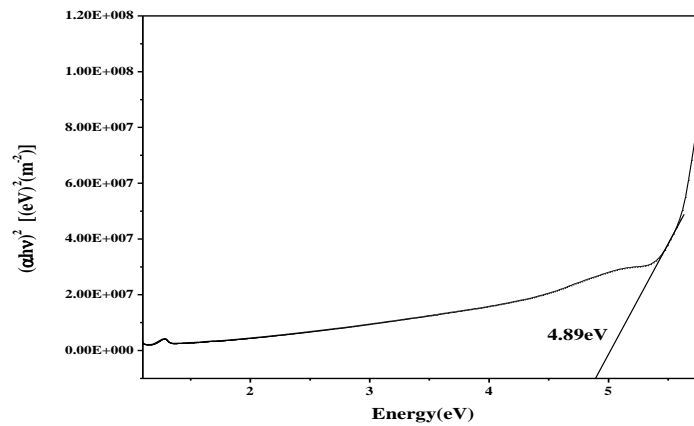
Figure.12. Energy band gap of LHHF
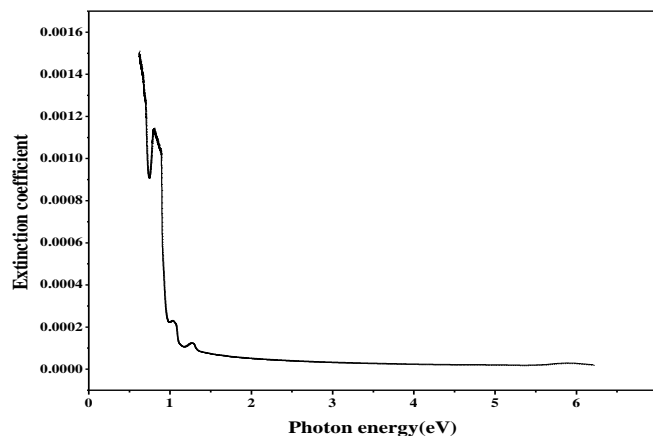
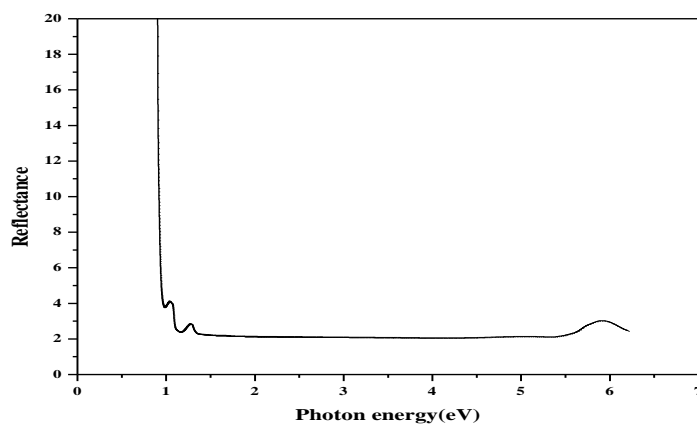**Figure .13. Extinction coefficient Vs Incident Photon Energy of LHHF**

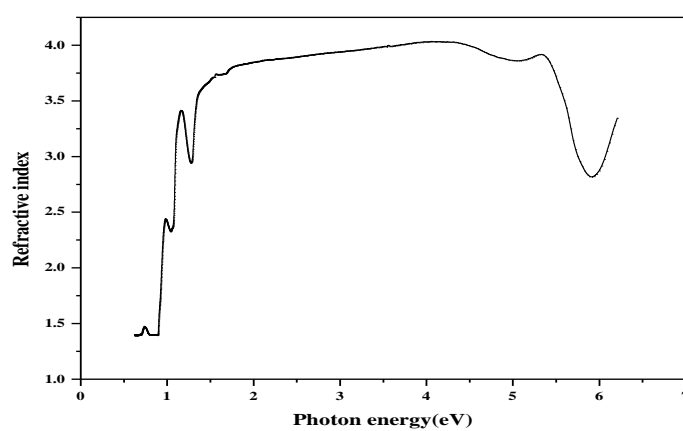**Figure.14. Reflectence Vs Incident photon energy of LHHF**

Figure .15. Refractive index Vs Incident photon energy of LHHF

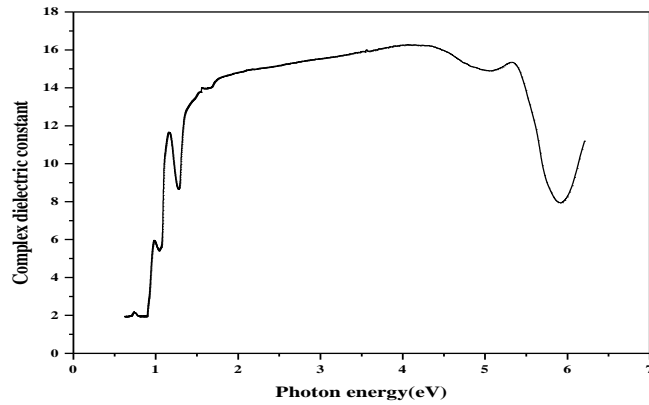**Figure .16. Complex dielectric constant Vs Incident photon energy of LHHF**
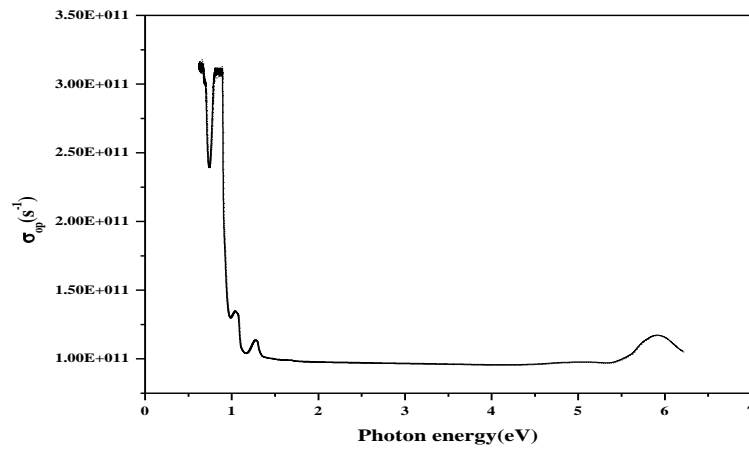

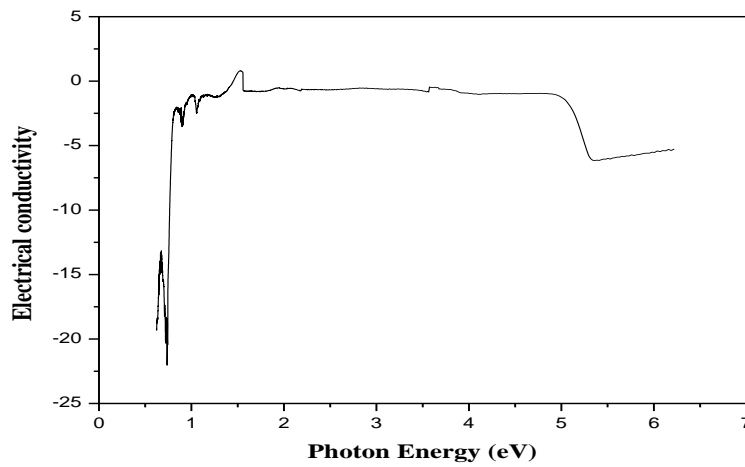**Figure.17. Optical conductivity Vs Incident photon energy of LHHF**

Figure.18. Electrical conductivity Vs Incident photon energy of LHHF

SHG EFFICIENCY

The second harmonic generation efficiency of the grown LHHF crystal was measured using standard Kurtz and Perry method. The grown crystals were ground and densely packed in a capillary tube. Nd:YAG laser of wavelength 1064 nm with pulse width of 8 ns and a repetition rate of 10 Hz was passed through the packed powder sample. Potassium The output of laser beam having bright green emission of wavelength 532 nm confirms the second harmonic generation. For a laser input pulse of 6.2 mJ, the second harmonic signal (532 nm) of 91.66 mW and 563.71 mW were obtained through reference KDP and grown LHHF samples respectively. Thus the SHG efficiency of LHHF is six times higher than that of KDP.

CONCLUSION

Single crystals of LHHF have been synthesized and grown from aqueous solution by slow evaporation technique at room temperature. Powder XRD studies show that the grown crystal belongs to orthorhombic crystal system having noncentro symmetry with $P2_12_12_1$ space group. Optimized structure of the isolated LHHF molecule obtained by DFT calculations give the minimum energy state. First order hyperpolarizability of LHHF is calculated as 5.91506×10^{-30} esu, 5.80467×10^{-30} esu using 6-31+ G (d, p) and 6-311++ G (d, p) respectively. It is also found useful in molecular designing. Theoretical and experimental Spectroscopic studies exemplify the presence of various functional groups in the molecule. The theoretically obtained FT-IR spectrum resembles the experimental pattern and the results are in close agreement. HOMO–LUMO orbital have been visualized and the Mulliken charges of the molecule were also calculated and interpreted. Frontier molecular orbital analyses give the HOMO-LUMO energy gap value as 4.178 and 4.260 eV. The UV-Vis absorption spectrum confirms that, the LHHF crystal possesses a wider transparency range in entire visible and near infra red region and the energy gap value of the grown crystal is 4.89 eV. SHG efficiency of the grown crystal shows that it is 6 times greater than KDP.

REFERENCES

[1]   Sahraoui B, Rivoire G, Terkia-Derdra N, Salle M, Zaremba J, J. Opt. Soc. Am. B, 1998; 15(2):923-928.
[2]   Ouazzani H. E, Iliopoulos K, Pranaitis M, Krupka O, Smokal V, Kolendo A, Sahraoui B, J. Phys. Chem. B 2011; 115: 1944-1949.
[3]   Indumathi N, Deepa K, Madhavan J, and Senthil S, Mechanics, Materials Science & Engineering, 2017; 9: Doi: 10.2412/mmse.5.76.497.
[4]   Madhavan J, Aruna S.K, Prabha J, Packium Julius , Ginson P Joseph ,Selvakumar S, Sagayaraj P, Journal of crystal growth, 2006; 293:409-414.
[5]   Tanak H, Koysal Y, Işik S, Yaman H, Ahsen V, Bull. Korean Chem. Soc, 2011;32(2): 673-680.
[6]   Vaschetto M. E, Retamal B. A, Monkman A. P, J. Mol. Struct. Theochem. 1999;468:209–221.
[7]   Timothy Clark, Jayaraman Chandrasekhar, Günther W. Spitznagel, Paul Von Ragué Schleyer, J. Comput. Chem. 1983;4: 294.
[8]   Scott Gronert, Chem. Phys. Letter, 1996; 252: 415–418.
[9]   Forsyth D. A, Sebag A. B, J. Am. Chem. Soc. 1997; 119: 9483–9494.
[10]   Petrosyan H. A, Karapetyan H. A, Yu M. Antipin and Petrosyan A. M, Journal of crystal Growth, 2005;275: 1919-1925.
[11]   Foresman J.B, Frish (Ed) E, Exploring chemistry with Electronic structure Methods: a Guide to using Gaussian, (Gaussian Inc., Pittsburg, PA, 1996).
[12]   Mulliken R.S, J. Chem. Phys. 23 (1955) 1833-1840.